Published OnlineFirst April 21, 2009; DOI: 10.1158/0008-5472.CAN-08-2747

Research Article

Doxorubicin and Paclitaxel-Loaded Lipid-Based Nanoparticles Overcome Multidrug Resistance by Inhibiting P-Glycoprotein and Depleting ATP

Xiaowei Dong,[1] Cynthia A. Mattingly,[1] Michael T. Tseng,[2] Moo J. Cho,[3] Yang Liu,[3] Val R. Adams,[1] and Russell J. Mumper[3,4]

[1]Department of Pharmaceutical Sciences, College of Pharmacy, University of Kentucky, Lexington, Kentucky; [2]Department of Anatomical Science/Neurobiology, School of Medicine, University of Louisville, Louisville, Kentucky; and [3]Division of Molecular Pharmaceutics, Center for Nanotechnology in Drug Delivery, UNC Eshelman School of Pharmacy and [4]UNC Lineberger Comprehensive Cancer Center, University of North Carolina at Chapel Hill, Chapel Hill, North Carolina

Abstract

To test the ability of nanoparticle formulations to overcome P-glycoprotein (P-gp)–mediated multidrug resistance, several different doxorubicin and paclitaxel-loaded lipid nanoparticles were prepared. Doxorubicin nanoparticles showed 6- to 8-fold lower IC_{50} values in P-gp–overexpressing human cancer cells than those of free doxorubicin. The IC_{50} value of paclitaxel nanoparticles was over 9-fold lower than that of Taxol in P-gp–overexpressing cells. A series of *in vitro* cell assays were used including quantitative studies on uptake and efflux, inhibition of calcein acetoxymethylester efflux, alteration of ATP levels, membrane integrity, mitochondrial membrane potential, apoptosis, and cytotoxicity. Enhanced uptake and prolonged retention of doxorubicin were observed with nanoparticle-based formulations in P-gp–overexpressing cells. Calcein acetoxymethylester and ATP assays confirmed that blank nanoparticles inhibited P-gp and transiently depleted ATP. I.v. injection of pegylated paclitaxel nanoparticles showed marked anticancer efficacy in nude mice bearing resistant NCI/ADR-RES tumors versus all control groups. Nanoparticles may be used to target both drug and biological mechanisms to overcome multidrug resistance via P-gp inhibition and ATP depletion. [Cancer Res 2009;69(9):3918–26]

Introduction

Drug resistance is the major cause of failure of cancer chemotherapy. Multidrug resistance (MDR) is a term used to describe the broad-spectrum resistance to chemotherapy in human cancer, which is a complex phenomenon that can result from several biochemical mechanisms that are still not fully understood (1). A widely studied mechanism of MDR is that resulting from altered cell membrane transport. P-glycoprotein (P-gp) encoded by the mdr1 gene is well-characterized and known to be a clinically important transporter protein belonging to the ATP-binding cassette family of membrane transporters (2). It has been shown to pump substrates, including doxorubicin and paclitaxel, out of tumor cells through an ATP-dependent mechanism that reduces the effective drug concentrations and consequently decreases the cytotoxic activity. A large number of P-gp inhibitors have been developed. However, clinical trials have been disappointing due to the high inherent toxicities of P-gp inhibitors and/or changed pharmacokinetics and biodistribution properties of anticancer drugs coadministrated with P-gp inhibitors (3).

Formulation strategies have been developed to potentially address P-gp–mediated resistance including colloidal delivery systems, polymer-drug conjugates, and polymeric-micelles. Certain drug-loaded liposomes (4, 5) and solid lipid nanoparticles (6, 7) have been shown to decrease the resistance of P-gp–expressing cells *in vitro*, which has been attributed to increased cellular accumulation of the drug. However, importantly, intracellular drug was still removed by P-gp efflux because formulations did not affect P-gp function (8, 9). Anticancer drugs conjugated to polymers such as *N*-(2-hydroxypropyl) methacrylamide have been shown to effectively kill both sensitive and resistant cancer cells. Proposed mechanisms for these conjugates in resistant cells include internalization by endocytosis, partial inhibition of P-gp gene expression (10), and modification of caspase-dependent apoptosis signaling pathways (11). Polymeric-micelles based on Pluronic® coblock polymers composed of poly(oxyethylene)-poly(oxypropylene) have been used to modulate P-gp in cancer cells (12, 13). Pluronic micelles have been used to selectively inhibit the P-gp efflux system by ATP depletion in P-gp cells, as well as to reduce the glutathione/glutathione S-transferase detoxification system and to alter apoptotic signal transduction.

Our laboratory has previously developed paclitaxel nanoparticles wherein the drug was entrapped into nanoparticles having emulsifying wax as the oil phase and polyoxyethylene 20-stearyl ether (Brij 78) as the surfactant. These paclitaxel nanoparticles were used to overcome P-gp–mediated resistance *in vitro* in a human colon adenocarcinoma cell line (HCT-15; ref. 14) and *in vivo* in a nude mouse HCT-15 xenograft model (15). The purpose of the present article was to determine how improved paclitaxel nanoparticles and new doxorubicin nanoparticles overcome P-gp–mediated resistance.

Materials and Methods

Tumor cell lines and cell culture. The P-gp–overexpressing human ovarian carcinoma cell line NCI/ADR-RES and sensitive cell line OVCAR-8 were both obtained from National Cancer Institute. The P-gp–overexpressing human melanoma cell line MDA-MB-435/LCC6MDR1 and matching sensitive cell line were kindly provided by Dr. Robert Clarke (Georgetown University, Washington, DC).

Preparation and characterization of doxorubicin and paclitaxel nanoparticles. Drug-loaded nanoparticles were prepared directly from warm o/w microemulsion precursors. Doxorubicin nanoparticles were prepared and characterized as previously described (16). Doxorubicin

Request for reprints: Russell J. Mumper, University of North Carolina Eshelman School of Pharmacy, University of North Carolina at Chapel Hill, Chapel Hill, NC 27599-7360. Phone: 919-966-1271; Fax: 919-966-0197; E-mail: mumper@email.unc.edu.

doi:10.1158/0008-5472.CAN-08-2747

Published OnlineFirst April 21, 2009; DOI: 10.1158/0008-5472.CAN-08-2747

release studies (n = 3) were completed at 37°C using the dialysis method. Doxorubicin nanoparticles (200 μL) in a cellulose ester dialysis membrane (MWCO: 100,000) were submerged in PBS (pH 7.4) at 37°C. Released doxorubicin was measured by fluorescence detection at 480 nm excitation and 550 nm emission. Paclitaxel nanoparticles were also prepared and characterized as previously described (17). To prepare pegylated paclitaxel BTM nanoparticles, Brij 700 (8% w/w ratio of Brij 700 to Miglyol 812) was added before cooling the microemulsion.

***In vitro* cytotoxicity studies.** Cells were seeded into 96-well plates at 1.5×10^4 cells per well and allowed to attach overnight. Cells were incubated for 48 h with drug equivalent concentrations of all test articles ranging from 10,000 nmol/L to 0.01 nmol/L of free drug (corresponding to 5.45 μg/mL–5.45 pg/mL for doxorubicin, and 8.54 μg/mL–8.54 pg/mL for paclitaxel). The sulforhodamine B assay was performed and IC_{50} values were calculated based on the percentage of treatment over control (18).

Cellular uptake and efflux of doxorubicin in cells. Cells were seeded in 48-well plates at a density of 2×10^5 cells per well and incubated overnight. Confluent cell monolayers were washed with Earle's balanced salt solution (EBSS) and treated with test articles. All samples were diluted with EBSS buffer and adjusted to 5 μg doxorubicin per milliliter or the doxorubicin equivalent concentration. Cells were treated with samples at 37°C for 0.5, 1, and 2 h. Cells were washed twice with ice-cold PBS (pH 7.4) and lysed with PBS containing 1% Triton X-100 at 37°C for 30 min. For efflux studies, cells were treated with each sample for 2 h, washed, and then cells were incubated with EBSS buffer at 37°C for another 1, 2, and 4 h. Doxorubicin concentrations in cell lysates were measured by HPLC on an Inertsil ODS-3 column with a mobile phase consisting of 0.1 mol/L ammonium formate containing 0.14% triethylamine [adjusted pH to 2.4 by addition of formic acid-acetonitrile-methanol-tetrahydrofuran (60:25:17.5:2.5, v/v/v/v) at a flow rate of 1.0 mL/min, and doxorubicin was detected by fluorescence with 480/550 nm excitation/emission. doxorubicin concentrations were normalized for protein content as measured with the BCA assay (Pierce; ref. 19)]. The cell efflux rate was calculated as (uptake at 2 h − efflux at 4 h)/4.

Calcein acetoxymethylester assay for P-gp function. A calcein acetoxymethylester (calcein AM) assay was performed using a modified method (20). Briefly, cells were seeded in black 96-well plates at a density of 1×10^5 cells per well overnight and treated with 50 μL of various doses of test articles diluted in EBSS buffer. After 0.5 h at 37°C, 50 μL of 0.25 μmol/L calcein AM (Sigma-Aldrich) were added into each well and the fluorescence of calcein was immediately measured every 5 min for 1 h using a microplate reader with 485/589 excitation/emission at room temperature. For pretreatment experiments, cells were exposed to blank NPs #2 for 0.5 h and washed, and then 50 μL of fresh EBSS buffer was added before addition of calcein AM. The % relative fluorescence (FL) in the cells was expressed as: % FL = $[(FL_{treatment} - FL_{nontreatment})/FL_{nontreatment}] \times 100\%$.

To assess cell membrane integrity, cells were treated with the same samples for 0.5 h at 37°C, and then incubated for 1 h at room temperature. Then, cells were trypsinized and 50 μL of 0.4% trypan blue solution was added. Membrane integrity was normalized to untreated control and expressed as (viable cells/total cells) × 100%.

ATP and apoptosis assays. An ATP assay was performed as described previously (21). Cells were seeded in 48-well plates at a density of 2×10^5 cells per well and incubated overnight. Various doses of test articles in EBSS buffer were added to cells and incubated at 37°C for 2 h. After treatment, cells were washed twice with ice-cold PBS and lysed with PBS containing 1% Triton X-100 at 37°C for 30 min. ATP in cell lysates was then measured using ATPlite 1step Assay kit (PerkinElmer) and normalized for protein content. Cell apoptosis under the tested conditions above was measured using the Annexin V-FITC Apoptosis Detection kit I (BD Biosciences).

Table 1.

A. Compositions of doxurubicin and paclitaxel nanoparticles

Formulations	Ion-pair	Oil phases (mg/mL)				Surfactants (mg/mL)	
		E. wax	Stearyl alcohol	Glyceryl tridodecanoate	Miglyol 812	TPGS	Brij 78
Dox NPs #1	STDC	2.0	—	—	—	2.6	2.0
Dox NPs #2	STS	2.0	—	—	—	2.6	2.0
Dox NPs #3	STS	2.0	—	—	—	—	4.0
Dox NPs #4	STS	—	2.0	—	—	—	4.0
PX G78 NPs	None	—	—	1.7	—	—	4.0
PX BTM NPs	None	—	—	—	2.5	1.5	3.5

B. Summary of the physicochemical properties of DOX nanoparticles and PX nanoparticles

Formulations	Mean diameter (nm)	% Drug loading (w/w drug/oil)	% Drug entrapment efficiency	% Drug released in 2 h
Dox NPs #1	102.3 ± 3.9	10	87.2	77.0 ± 1.1
Dox NPs #2	103.3 ± 1.2	15	86.2 ± 5.6	45.5 ± 7.1
Dox NPs #3	84.9 ± 3.3	15	91.0 ± 5.9	56.9 ± 2.4
Dox NPs #4	68.8 ± 2.5	15	91.8 ± 4.6	52.8 ± 2.4
PX G78 NPs	138.7 ± 1.3	7.5	85.4 ± 3.3	5.5 ± 1.1
PX BTM NPs	177.3 ± 1.4	6	97.5 ± 2.6	8.7 ± 4.0

NOTE: Final concentrations of doxorubicin and paclitaxel in drug-loaded nanoparticles were 300 and 150 μg/mL, respectively.
Abbreviations: Dox, doxurubicin; PX, paclitaxel; E. wax, emulsifying wax; NP, nanoparticles.

Published OnlineFirst April 21, 2009; DOI: 10.1158/0008-5472.CAN-08-2747

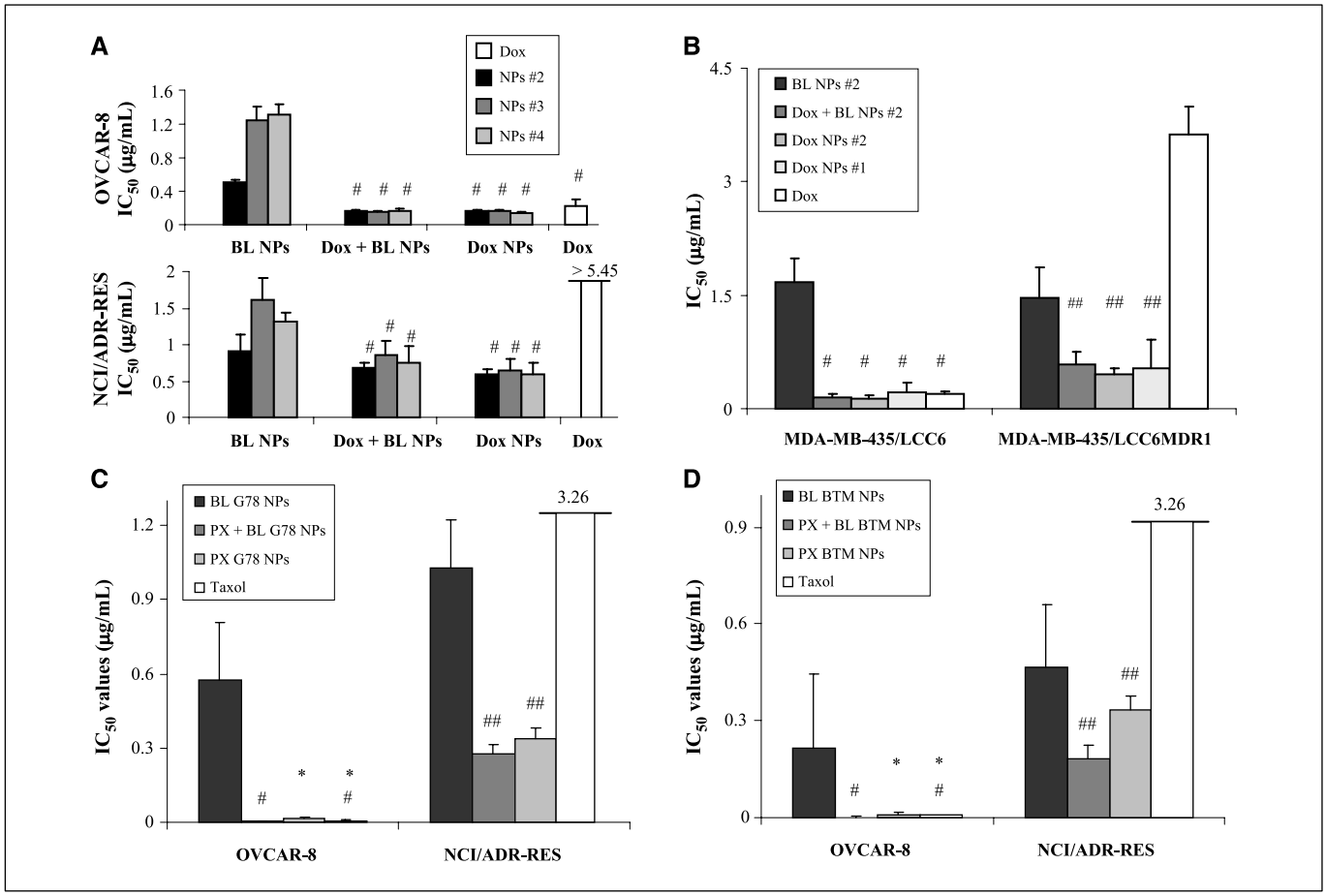

Figure 1. Doxorubicin (*Dox*) and paclitaxel (*PX*) cytotoxicity studies at 48 h. IC_{50} values (μg/mL) of doxorubicin and doxorubicin nanoparticles in (*A*) OVCAR-8 and NCI/ADR-RES cells and (*B*) MDA-MB-435/LCC6 and MDA-MB-435/LCC6MDR1 cells. *C,* IC_{50} values (μg/mL) of paclitaxel and paclitaxel G78 nanoparticles in OVCAR-8 and NCI/ADR-RES cells. *D,* IC_{50} values (μg/mL) of paclitaxel and paclitaxel BTM nanoparticles in OVCAR-8 and NCI/ADR-RES cells. *Columns,* mean of three independent experiments ($n = 3$) with triplicate ($n = 3$) measurements for each experiment; *bars,* SD. *, $P < 0.05$; # and ##, $P > 0.05$. "Drug equivalent doses" of nanoparticles and excipients are calculated from the composition shown in Table 1.

To assess whether cells could recover from ATP depletion, cells were incubated with various concentrations of test articles for 2 h, washed, and then incubated for another 4 and 13 h, and then ATP levels and total proteins were measured.

Histology studies by TEM. Cells were washed, scraped, and fixed in 4% buffered formalin, postfixed in 2% osmium tetraoxide, and dehydrated in ascending concentrations of ethanol before embedded in Araldite 502. Blocks were sectioned at 1 μm and 800 Å for light and electron microscopy. Thin sections were stained with lead citrate and uranyl acetate before examined using a Philips 10 electron microscope operated at 60 kV.

Mitochondrial potential measurement. Cells were seeded in black 96-well plates at a density of 1×10^5 cells per well overnight and treated with test articles for 2 h at 37°C. After washing, mitochondrial potential was detected using the JC-1 Mitochondrial Membrane Potential Detection kit (Biotium). Paclitaxel BTM nanoparticles (1.5 or 0.15 μg/mL) and 6 μg/mL of cyclosporin A were used as positive and negative controls. Mitochondrial potential was expressed as (red FL/green FL) $_{\text{treatment}}$/(red FL/green FL) $_{\text{nontreatment}} \times 100\%$.

3-(4,5-Dimethylthiazol-2-yl)-2,5-diphenyltetrazolium bromide assay. Resistant cells and their sensitive parental cells were seeded in 96-well plates as a density of 4×10^4 overnight and incubated with 3-(4,5-dimethylthiazol-2-yl)-2,5-diphenyltetrazolium bromide (MTT), and samples for 2 h at 37°C. Two hundred microliters of reagent containing 20% SDS, and 50% dimethyl formamide in water was added and incubated for 1 h at room temperature, and plates were read at 570 nm (test) and 650 nm (reference).

***In vivo* anticancer efficacy study using pegylated paclitaxel BTM nanoparticles.** Female nude (nu/nu) mice, 4 to 5 wk (Harlan Laboratories), were housed in a pathogen-free room. All experiments involving the mice were carried with an approved protocol by the University of North Carolina Animal Care and Use Committee. The mice were injected s.c. in the interscapular region with 4×10^6 NCI/ADR-RES cells suspended in DMEM. When the tumors exhibited volume between 50 and 150 mm^3, the mice were randomly assigned to different treatments at 2 different paclitaxel doses of 4.5 and 2.25 mg/kg. Mice were injected with either 100 or 200 μL of isotonic treatment article by i.v. injection. Tumors were measured in 2 perpendicular dimensions every 2 d for 12 d, and the tumor volume was calculated using the formula $V = (L \times W^2) / 2$, where L and W are the longest and shortest diameters, respectively.

Statistical analysis. Statistical comparisons were made with ANOVA followed by pair-wise comparisons using Student's t test using GraphPad Prism software. Results were considered significant at 95% confidence interval ($P < 0.05$).

Results

Doxorubicin and paclitaxel nanoparticles. The compositions and physicochemical properties of doxorubicin and paclitaxel nanoparticles are shown in Table 1*A* and *B*, respectively. Paclitaxel could be entrapped directly into G78 nanoparticles and BTM

Published OnlineFirst April 21, 2009; DOI: 10.1158/0008-5472.CAN-08-2747

nanoparticles. Doxorubicin ion-pair complexes with sodium taurodeoxycholate (STDC) were somewhat soluble in PBS that led to increased rates of doxorubicin release from the nanoparticles. In comparison, sodium tetradecyl sulfate (STS) fully precipitated doxorubicin at a mole ratio of 1:1.2 (doxorubicin/STS) and resulted in an ion-pair complex that had both low solubility in PBS and high solubility in the melted oil phases. All nanoparticles were stable over 1 month at 4°C (data not shown).

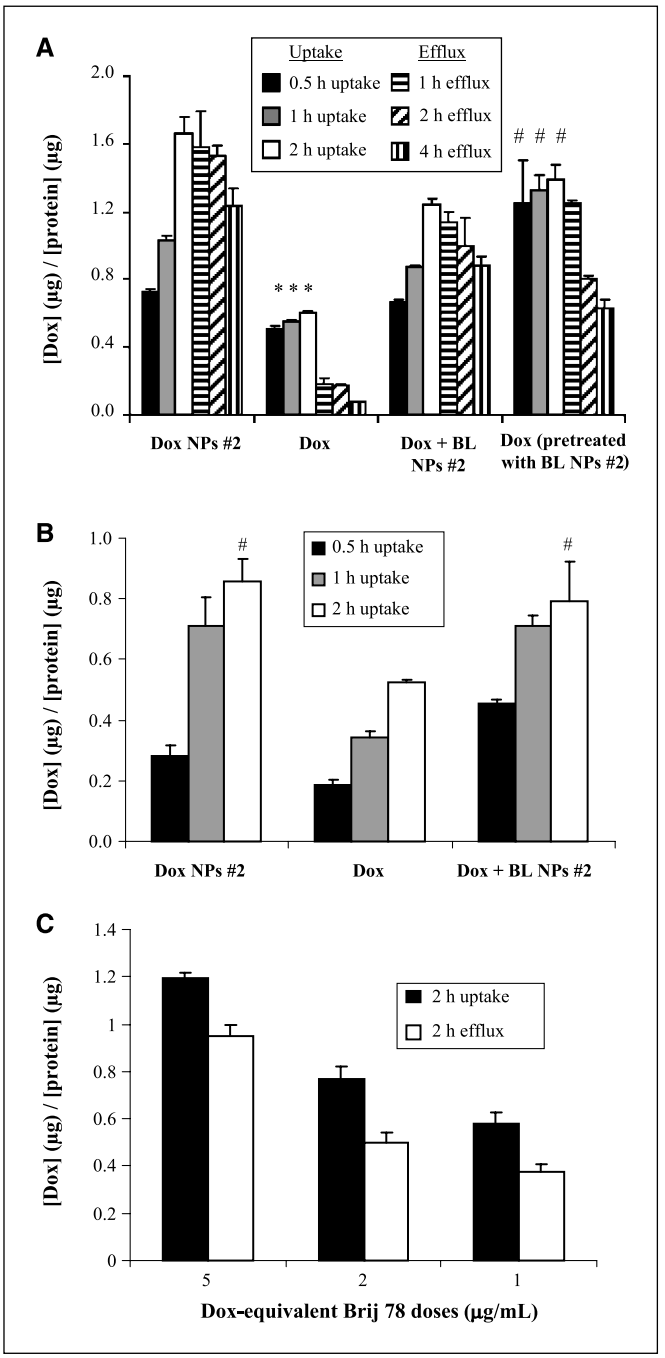

Figure 2. Cellular uptake and efflux of doxorubicin in NCI/ADR-RES and MDA-MB-468 cells. *A,* uptake and efflux in NCI/ADR-RES cells at 37°C, and (*B*) uptake in MDA-MB-468 cells at 37°C. For pretreatment experiments, cells were pretreated with blank NPs #2 for 0.5 h before the next step. For efflux studies, cells were treated with samples for 2 h, and then reincubated with fresh EBSS buffer for indicated time. *C,* doxorubicin uptake and efflux when cells were pretreated with Brij 78 at concentrations of 45.3, 18.1, and 9.1 μg/mL (corresponding to doxorubicin-equivalent doses of 5, 2, and 1 μg/mL, respectively) for 0.5 h. *Columns,* mean (n = 3); *bars,* SD. *, $P < 0.05$; #, $P > 0.05$.

***In vitro* cytotoxicity studies.** Cytotoxicity data in two pairs of parental (sensitive) and P-gp cell lines are reported in Fig. 1. As expected, in the tested doxorubicin concentration range, free doxorubicin showed no toxicity in NCI/ADR-RES cell line in the tested concentration range (IC_{50}, >5.45 μg/mL, corresponding to >10,000 nmol/L) and very low toxicity in MDA-MB-435/LCC6MDR1 cell line (IC_{50}, 3.62 μg/mL, corresponding to 6,643 nmol/L; Fig. 1*A* and *B*). Doxorubicin-loaded nanoparticles showed a clear dose-dependent cytotoxicity against all tested cell lines. In sensitive cell lines, the IC_{50} values of doxorubicin-loaded nanoparticles were comparable with those of free doxorubicin. In comparison, the IC_{50} values of doxorubicin NPs #2 were 8-fold lower in NCI/ADR-RES cells (IC_{50}, <0.61 μg/mL, corresponding to 1,111 nmol/L) and in MDA-MB-435/LCC6MDR1 cells (IC_{50}, <0.45 μg/mL, corresponding to 821 nmol/L) than those of free doxorubicin. Blank nanoparticles did not cause significant cytotoxicity against all cell lines up to a total nanoparticle dose of 30 μg/mL.

Interestingly, the postaddition of doxorubicin to blank nanoparticles showed similar cytotoxicity to doxorubicin nanoparticles in both sensitive and resistant cell lines. Thus, to ascertain if this phenomenon was drug specific, paclitaxel G78 nanoparticles and paclitaxel BTM nanoparticles were tested for cytotoxicity in OVCAR-8 and NCI/ADR-RES cells and compared with Taxol. As shown in Fig. 1*C* and *D*, the IC_{50} value of Taxol in NCI/ADR-RES cells was 495-fold greater (IC_{50}, 3.26 μg/mL, corresponding to 3,814 nmol/L) than that in sensitive cells (IC_{50}, 0.00658 μg/mL, corresponding to 7.7 nmol/L). Also, the IC_{50} value of both paclitaxel nanoparticles was over 9-fold lower than that of Taxol in P-gp cells. Both blank nanoparticles did not show significant cytotoxicity in these cell lines. Similar to when free doxorubicin was post-added to blank nanoparticles, the postaddition of free paclitaxel to blank G78 nanoparticles or blank BTM nanoparticles had comparable cytotoxicity to that of paclitaxel entrapped in nanoparticles. The IC_{50} values of the postaddition were slightly lower than those of paclitaxel nanoparticles in both cell lines; however, the difference was statistically significant ($P < 0.05$) only in the sensitive cells.

Cellular uptake and efflux of doxorubicin. The uptake and efflux of doxorubicin with various formulations containing 5 μg/mL of doxorubicin was examined in both NCI/ADR-RES and MDA-MB-468 cells at different temperatures (Fig. 2). Doxorubicin NPs #2 were chosen as the basic nanoparticle formulation for these studies. The uptake of doxorubicin was time dependent except when cells were pretreated with blank NPs #2. In NCI/ADR-RES cell line at 37°C, nanoparticles led to over a 2-fold increase in the extent of uptake compared with treatment with free doxorubicin (Fig. 2*A*). Similarly, all treatments with nanoparticle formulations enhanced the retention of doxorubicin. After cells were treated with doxorubicin NPs #2, >15-fold doxorubicin remained in the P-gp cells and the efflux rate was 1.5-fold lower compared with free doxorubicin after 4 hours of efflux. Importantly, the postaddition of doxorubicin to blank NPs #2 also showed enhanced uptake and retention. To eliminate the possibility that doxorubicin was quickly bound to the surface of blank NPs #2, cells were pretreated with blank NPs #2 and washed before the addition of free doxorubicin. In this treatment, the uptake of doxorubicin was very rapid and reached a maximum within 0.5 hour, and 7-fold greater doxorubicin was retained in cells compared with free doxorubicin.

Published OnlineFirst April 21, 2009; DOI: 10.1158/0008-5472.CAN-08-2747

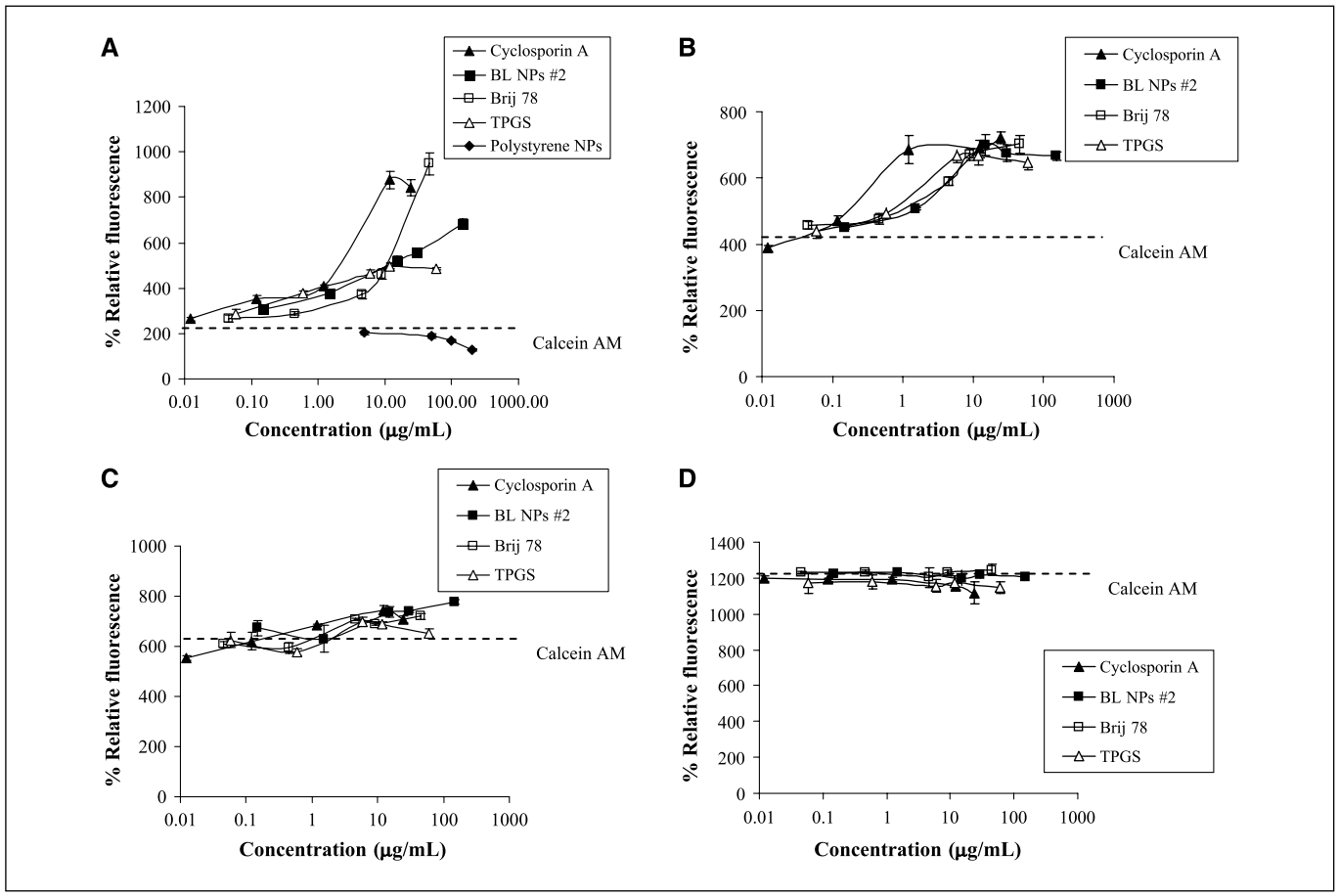

Figure 3. Dose response of blank NPs #2 and surfactants in calcein AM assay in NCI/ADR-RES cells (*A*), MDA-MB-435/LCC6MDR1 cells (*B*), OVCAR-8 cells (*C*), and MDA-MB-435/LCC6 cells (*D*). Concentrations are presented as concentrations of blank NPs #2 (sum of mass of oils and surfactants) and as concentrations of free Brij 78 and TPGS. *Points,* mean (n = 3); *bars,* SD.

However, the efflux rate of this treatment [0.19 (doxorubicin)(ng)/(protein)(μg)/h] was significantly greater than that of free doxorubicin [0.13 (doxorubicin)(ng) / (protein)(μg)/h; $P < 0.05$; Fig. 2*A*]. The uptake of doxorubicin in NCI/ADR-RES cells at 4°C with doxorubicin NPs #2 and free doxorubicin was 24-fold lower and 10-fold lower, respectively, than those at 37°C. Unlike the uptake at 37°C that showed marked differences between nanoparticle groups and free doxorubicin, the differences at 4°C were significantly reduced (data not shown). The extent of doxorubicin uptake was also carried out in sensitive MDA-MB-468 cells at 37°C. Nanoparticle formulations showed greater uptake than free doxorubicin as shown in Fig. 2*B*. In fact, the doxorubicin NPs #2 very rapidly entered MDA-MB-468 cells and doxorubicin from nanoparticles quickly and extensively localized inside the nuclei of cells by fluorescence microscopy (data not shown).

To confirm that Brij 78 could also enhance doxorubicin uptake and decrease efflux, NCI/ADR-RES cells were pretreated with various concentrations of Brij 78 (Fig. 2*C*). At the concentrations of Brij 78 that showed ATP depletion, pretreatment of cells with Brij 78 led to comparable doxorubicin uptake enhancement and efflux reduction compared with blank NPs #2 (Fig. 2*A*).

Calcein AM assay. The ability of blank NPs #2, and the Brij 78 and d-α-tocopherol polyethylene glycol 1000 succinate (TPGS) surfactants to inhibit P-gp was evaluated using the calcein AM assay in five resistant and sensitive cell lines (Fig. 3). Under all conditions tested, the trypan blue assay confirmed that there was no significant loss of cell membrane integrity (data not shown). In resistant cells, the fluorescence caused by intracellular calcein significantly increased in a dose-dependent manner either in the presence of blank BTM nanoparticles (data not shown), blank NPs #2 (Fig. 3*A* and *B*), or when cells were pretreated with blank NPs #2 for 0.5 hour (data not shown). Brij 78 and TPGS surfactants also led to a dose-dependent increase in calcein fluorescence over 1 hour. In contrast, polystyrene nanoparticles did not increase intracellular fluorescence. In stark contrast, no treatments led to increased intracellular fluorescence compared with calcein AM alone in the sensitive MDA-MB-468 cells (data not shown), OVCAR-8 cells (Fig. 3*C*), and MDA-MB-435/LCC6 cells (Fig. 3*D*). However, the human melanoma MDA-MB-435/LCC6 cells showed greater permeability as the uptake of calcein AM was higher in these cells.

ATP and apoptosis assays. To further understand the mechanisms by which blank nanoparticles and surfactants inhibited P-gp, intracellular ATP levels in cells were measured after exposure to various concentrations of blank NPs #2, Brij 78, and TPGS. In resistant NCI/ADR-RES and MDA-MB-435/LCC6MDR1 cells, ATP levels decreased in a dose-dependent manner after treatment with blank BTM nanoparticles, blank NPs #2, and Brij 78% to 40%, 35%, and 20% of the initial value, respectively; however, there was no change in ATP levels after treatment with TPGS (Fig. 4*A*). Importantly, cyclosporin A and

Published OnlineFirst April 21, 2009; DOI: 10.1158/0008-5472.CAN-08-2747

polystyrene nanoparticles did not decrease ATP levels in the tested concentration range in NCI/ADR-RES cells. In contrast, over all tested concentrations in sensitive MDA-MB-468 and OVCAR-8 cells, only 0.5 and 1 μg/mL of Brij 78 and blank NPs #2 (doxorubicin equivalent doses) decreased ATP levels to 86% and 65% of the initial value, respectively (data not shown). However, ATP levels decreased in MDA-MB-435/LCC6 cells, which had no significant difference with those in corresponding resistant cells (data not shown). Also, TPGS decreased ATP levels in this sensitive cell line (data not shown). In the presence of 17 μg/mL of cyclosporin A, ATP levels further decreased by an additional 20% to 40% at each concentration tested (data not shown). Finally, ATP recovery studies showed that after blank NPs #2 and Brij 78 were removed from NCI/ADR-RES cells, cellular ATP levels returned to 100% after 4 hours for the lower concentrations tested and were completely restored after 13 hours for all concentrations (Fig. 4*B*).

Under the conditions analogous to the ATP depletion experiments, 4 concentrations of doxorubicin-equivalent doses (0.5, 1, 2, and 5 μg/mL) for the Brij 78 and TPGS surfactants and blank nanoparticles were tested for their ability to induce apoptosis versus control cells at 2 hours in NCI/ADR-RES cells. Only blank nanoparticles at 5 μg/mL showed significance versus control ($P < 0.05$), and these differences were modest (8% versus 6.7% for control).

Transmission electron microscopy. MDA-MB-468, OVCAR-8, and NCI/ADR-RES cells are anchorage-dependent epitheloid cells. The effects of doxorubicin on these cells seemed similar with the major changes in the degree of nuclear chromatin compaction. In

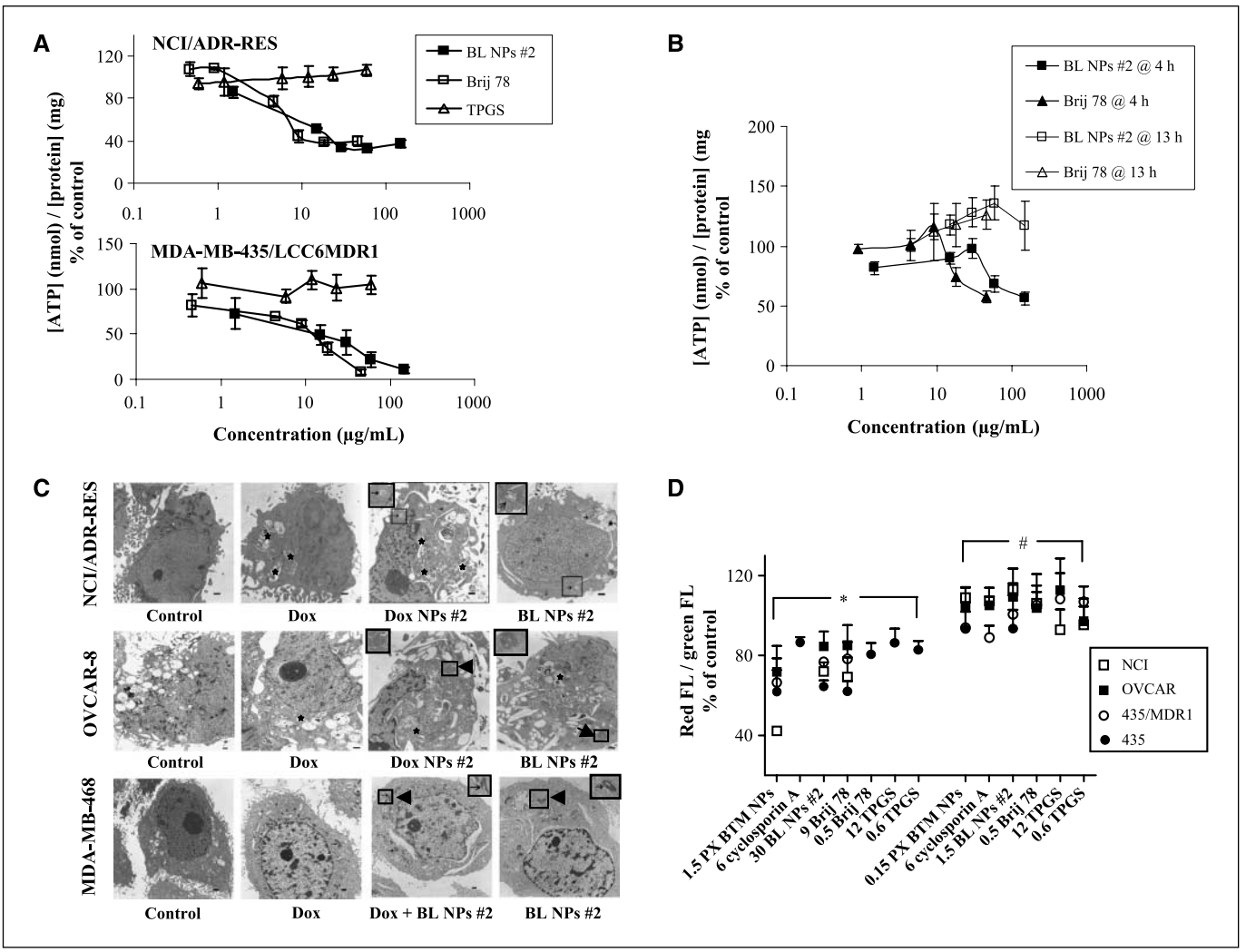

Figure 4. The effects of nanoparticles on ATP levels and mitochondria. *A,* effect of blank NPs #2 and surfactants on intracellular ATP level in NCI/ADR-RES cells and MDA-MB-435/LCC6MDR1 cells. *B,* ATP recovery in NCI/ADR-RES cells for 4 and 13 h. Cells were treated with test samples for 2 h at 37°C and then samples were removed from cells. Cellular ATP levels were measured after cells were continuously incubated in fresh medium for another 4 and 13 h. Concentrations are presented as concentrations of blank NPs #2 (sum of mass of oils and surfactants) and as concentrations of free Brij 78 and TPGS. *Points,* mean ($n = 3$); *bars,* SD. *, $P < 0.05$; #, $P > 0.05$. *C,* transmission electron microscopy analysis in NCI/ADR-RES, OVCAR-8, and MDA-MB-468 cells treated with doxorubicin NP #2, free doxorubicin, blank NP #2. Cells were treated for 1 h with samples containing doxorubicin equivalent dose at 5 μg/mL. Treatment with doxorubicin NPs #2, blank NP #2 caused considerable mitochondria swelling in NCI/ADR-RES and OVCAR-8 cells but not in MDA-MB-468 cells. *, multivesicular bodies; →, mitochondria. *Scale bar,* 1 μm. *D,* mitochondrial potential measurement in NCI/ADR-RES cells and MDA-MB-435/LCC6MDR1 cells and their corresponding parental cells. Cells were treated with samples for 2 h at 37°C. Mitochondrial potential detection was based on the ratio of red fluorescence (*FL*) caused by the accumulation of JC-1 in mitochondria and green fluorescence caused by the accumulation of JC-1 in the cytoplasm. The number before each label on x-axis indicates the concentration of tested samples (μg/mL).

Published OnlineFirst April 21, 2009; DOI: 10.1158/0008-5472.CAN-08-2747

NCI/ADR-RES and OVCAR-8 cells, doxorubicin NPs #2 or blank NPs #2 treatment induced the most severe changes that included cytoplasmic accumulation of multivesicular bodies, chromatin condensation, and varying degree of mitochondrial swelling. After 1 hour of incubation, swollen mitochondria were frequently observed in the resistant cells treated with doxorubicin NPs #2 or blank NPs #2 (Fig. 4*C*). However, this effect was not observed in the sensitive MDA-MB-468 cells. In comparison, Brij 78 also produced mitochondrial swelling in NCI/ADR-RES and OVCAR-8 cells (data not shown). In human melanoma cells, MDA-MB-435/LCC6 and MDA-MB-435/LCC6MDR1, swollen mitochondria were also observed with the treatment of blank NPs #2 or Brij 78 (data not shown).

Mitochondrial potential measurement. Mitochondrial potential changed in all tested cells treated with blank NPs #2 and Brij 78 at the same concentrations that depleted ATP (Fig. 4*D*). TPGS did not change mitochondrial potential in all cell lines except in MDA-MDB-435/LCC6. All tested samples changed mitochondrial potential in MDA-MB-435/LCC6 cells except the treatment with 0.15 μg/mL of paclitaxel BTM nanoparticles.

MTT assay. To a certain extent, all tested samples including blank NPs #2, Brij 78, and TPGS decreased MTT reduction in a dose-dependent manner, except at the lowest concentration of tested samples (0.05 μg/mL of doxorubicin equivalent dose) (data not shown). The minimum value of MTT reduction at 1 μg/mL of doxorubicin equivalent dose was 71% ± 8% (versus control) and observed in MDA-MB-435/LCC6 cells treated with blank NPs #2 (30 μg/mL).

***In vivo* anticancer efficacy study.** Tumor volume increased with control, Taxol, and blank BTM NPs administration at the two paclitaxel or paclitaxel-equivalent doses tested. In comparison, a marked anticancer effect of the pegylated paclitaxel BTM nanoparticles was clearly observed (Fig. 5). The tumor volume in the two tested pegylated paclitaxel BTM nanoparticles groups almost did not change during the course of the study. A statistically significant difference of pegylated paclitaxel BTM nanoparticles from all other treatments was observed from day 5 and continued to the end of the study. Blank BTM nanoparticles did not show any clinical signs of toxicity even at the highest dose of 210-mg nanoparticles/kg.

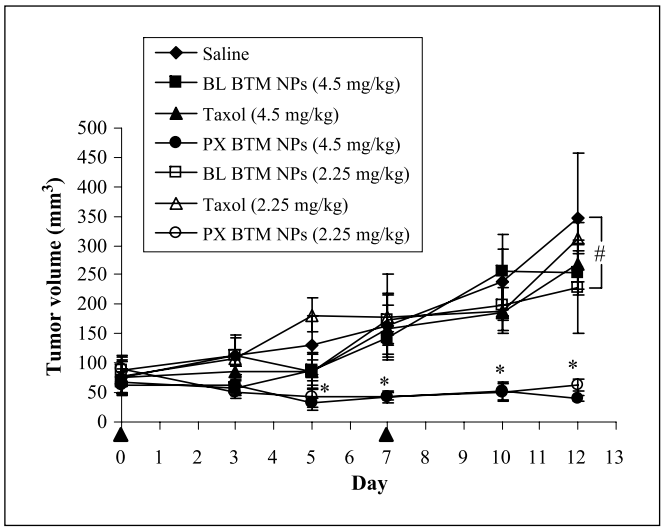

Figure 5. *In vivo* anticancer efficacy studies using pegylated paclitaxel BTM nanoparticles in resistant mouse NCI/ADR-RES xenografts. Female nude mice (18–19 g) received 4 × 10^6 cells by s.c. injection. Mice (n = 4 per group) were dosed i.v. with paclitaxel (4.5 or 2.25 mg/kg) by tail vein injection on day 0 and 7. The corresponding nanoparticle dose was 210 or 105 mg nanoparticles/kg, respectively. *Points,* mean; *bars,* SD.

Discussion

The objective of the present studies was to investigate the potential of drug-loaded lipid nanoparticles to overcome P-gp–mediated drug resistance, and to elucidate possible mechanisms. The results of the cytotoxicity studies indicate that all tested drug-loaded nanoparticles significantly reduced IC_{50} values in P-gp–overexpressing ovarian and melanoma cell lines over free drug. Of interest was that the postaddition of free doxorubicin to blank nanoparticles also showed similar IC_{50} values compared with doxorubicin-loaded nanoparticles (Fig. 1). This is a similar observation as reported by Némati and colleagues (22) in which doxorubicin-loaded polyalkylcyanoacrylate nanoparticles were used to treat sensitive and resistant leucemic murine cells. This observation could be the result of two possibilities: (*a*) due to strong adhesive properties, doxorubicin is adsorbed onto the surface of nanoparticles (23), and (*b*) blank nanoparticles could affect P-gp and therefore enhance the cytotoxicity of doxorubicin. To test these two possibilities, paclitaxel was used because the neutral paclitaxel would be less likely to adhere to the slightly negatively charged nanoparticles. In a similar manner as doxorubicin nanoparticles, free paclitaxel postadded to blank nanoparticles showed comparable cytotoxicity as paclitaxel-loaded nanoparticles. Temperature-dependent uptake of doxorubicin NPs #2 in NCI/ADR-RES cells indicates an endocytosis pathway of nanoparticles uptake. Obviously, nanoparticles not only enhanced the uptake of doxorubicin but also improved the retention of doxorubicin in resistant cell lines even if doxorubicin was entrapped into nanoparticles or physically present with blank nanoparticles. More importantly, the uptake and retention of doxorubicin increased when cells were pretreated with blank nanoparticles or free Brij 78 and then free doxorubicin was added (Fig. 2*A* and *C*). These results are in contrast to a previous study that showed that the uptake and retention of doxorubicin in MDA-MB-435/LCC6MDR1 cells were not improved when free doxorubicin was added to polymer-lipid hybrid nanoparticles (8). These contrasting studies seem to indicate a different and preferential mechanism of our nanoparticles from the polymer-lipid hybrid NPs on P-gp. Taken as a whole, these studies prove that the lipid-based nanoparticles described in the present studies inhibit the function of P-gp. Although a prior study suggested that an ion-pair complex of doxorubicin and polycyanoacrylic acid, a degradation product of polyalkylcyanoacrylate nanoparticles, may increase the intracellular diffusion of doxorubicin and result in increased efficacy of doxorubicin nanoparticles in resistant cells (24), the present study suggested that the ion-pairing agents likely did not affect P-gp directly because the IC_{50} of paclitaxel nanoparticles prepared without ion-pair agents was also low (Fig. 1*C* and *D*). According to the data, the factor that was the most influential was the inclusion of the surfactant Brij 78 but not necessarily TPGS. In fact, it has been shown that some surfactants reverse the activity of P-gp and MRP2 (25). In these studies, we showed that both Brij 78 and TPGS were able to increase calcein AM influx in P-g cells, but only Brij 78 was found to deplete ATP. Calcein AM is a nonfluorescent substrate of P-gp that, once in the cells, is irreversibly converted by cytosolic esterase to calcein, a nonpermeable and fluorescent

Published OnlineFirst April 21, 2009; DOI: 10.1158/0008-5472.CAN-08-2747

molecule. Thus, the increased intracellular fluorescence of calcein when P-gp cells were exposed to lipid-based nanoparticles indicates the inhibition of P-gp function. Moreover, the integrity of membrane confirmed that the inhibition resulted from a selective interaction with P-gp rather than an unspecific membrane alteration, which may increase doxorubicin transport in resistant cells. Additionally, the inhibition of P-gp by blank nanoparticles was not related to nanoparticle size because polystyrene nanoparticles having the same particle size had no effect on the intracellular fluorescence (Fig. 3*A*). Because P-gp efflux is an energy-dependent process, intracellular ATP levels were investigated. The results of the present studies show that exposure to blank NPs #2 induces a significant decrease in ATP levels in two resistant cells without inducing cell apoptosis. The effect of individual surfactant on ATP levels also was examined. It is clear that Brij 78, not TPGS, decreased ATP levels in resistant cell lines (Fig. 4*A*). Even at a very low actual concentration of 4.5 μg/mL, which is well below the critical micelle concentration of Brij 78 (860 μg/mL), Brij 78 reduced the ATP levels after 2 hours to 78% of the initial value. The ATP levels in sensitive cells responded differently to different cells. ATP levels only slightly changed in MDA-MB-468 and OVCAR-8 cells, whereas ATP levels in MDA-MB-435/LCC6 cells decreased to the same extent as with the corresponding resistant cells after treatment with either blank NPs #2 or Brij 78. Our findings on ATP depletion are in agreement with the previous reports from the Kabanov group that concluded that ATP depletion caused by Pluronic P85 block copolymer was one of the major reasons for reversal P-gp activity and dominant in P-gp cells (20, 26). Moreover, Brij 78 had similar influence on enhanced doxorubicin uptake and retention compared with blank NPs #2 (Fig. 2*C*). The results of the present study also suggested that reversal of P-gp function by ATP depletion caused by nanoparticles was transient and reversible, based on ATP recovery studies (Fig. 4*B*) and uptake and efflux studies (Fig. 2*A* and *C*).

Our previous studies suggested that Brij 78 could influence the activity of an alcohol dehydrogenase/NAD+ enzyme system *in vitro* (27). The mitochondria are responsible for regulation of cellular metabolism, and also are the ATP factory in cells. Increase in matrix volume of mitochondria can be due to energetic stress inside cells (28, 29). It is important to note that the MTT reduction may not result from cell death because the apoptosis data and ATP recovery data showed that cells did not undergo apoptosis and that the ATP depletion was transient. Therefore, the MTT assay data more likely suggested a change in the cell metabolic activity or enzyme activity in the mitochondrial respiratory chain in treated cells (30, 31). Therefore, it is likely that the metabolic activity was decreased in all cells treated with blank NPs #2 and Brij 78. Moreover, mitochondrial potential in resistant and sensitive cell lines changed at the same concentrations of blank NPs #2 or Brij 78 that depleted ATP. However, the change in mitochondrial potential and mitochondrial swelling did not destroy mitochondrial function as ATP levels returned to normal within 4 to 13 hours depending on the dose (Fig. 4*B*). It is worthy to note that MDA MB-435/LCC6 cells showed both changes in ATP levels and mitochondrial potential. These effects may be related to the high permeability of the cell membrane as observed by the relatively high uptake of calcein AM (Fig. 3*D*). The change in the mitochondrial potential was correlated with mitochondrial swelling in all tested cells in these studies. Thus, it is possible that Brij 78 and nanoparticles influence the enzymes involved in mitochondrial respiratory chain, and consequently produce energy stress in cells. As a consequence, the mitochondrial potential changes and the mitochondria swell to meet the energy requirement. These effects are likely pronounced in Pgp-overexpressing cells as they require more energy for P-gp expression and function.

The current study suggested that there are at least two major reasons for enhanced cytotoxicity of doxorubicin or paclitaxel-loaded lipid-based nanoparticles in P-gp–mediated resistant cells: (*a*) increased extent of drug uptake by endocytosis of nanoparticles, which helps to partially bypass P-gp; (*b*) decreased efflux rate of drug through inhibition of P-gp function and ATP depletion caused by Brij 78, a component of nanoparticles. Both increase intracellular drug concentrations, which is the key to overcoming transporter-mediated resistance. *In vivo* anticancer efficacy in mice bearing resistant NCI/ADR-RES cell xenografts showed that pegylated paclitaxel BTM nanoparticles significantly inhibited tumor growth versus all tested controls. The BTM nanoparticles also showed the ability to inhibit P-gp function and deplete ATP. Additional *in vivo* studies are on-going including pharmacokinetic and biodistribution studies, as well as additional efficacy studies in resistant and sensitive tumor mouse tumor models.

In conclusion, both doxorubicin and paclitaxel-loaded lipid-based nanoparticles containing the Brij 78 surfactant were shown to overcome P-gp–mediated drug resistance. The mechanism of P-gp inhibition and ATP depletion distinguishes these Brij 78-based nanoparticles from other known nanoparticles and liposome-based carrier systems. To the best of our knowledge, this is the first report on nanoparticles that can inhibit P-gp efflux and deplete ATP. Most importantly, nanoparticle-based carriers that effectively target both the drug and biological mechanisms to overcome MDR (P-gp inhibition and ATP depletion) seem to be a novel therapeutic strategy and additional *in vivo* work is warranted.

Disclosure of Potential Conflicts of Interest

R.J. Mumper is a founder of NanoMed Pharmaceuticals and currently sits as a member of the Board of Directors. NanoMed has some exclusive commercial rights to some of the nanoparticle technology described in this article. However, NanoMed did not fund any of the present research. No other co-author on this article has a potential conflict of interest.

Acknowledgments

Received 7/18/08; revised 1/28/09; accepted 2/18/09; published OnlineFirst 4/21/09.

Grant support: NIH-NCI R01 CA115197 (R.J. Mumper, V. Aadams, and M. Tseng).

The costs of publication of this article were defrayed in part by the payment of page charges. This article must therefore be hereby marked *advertisement* in accordance with 18 U.S.C. Section 1734 solely to indicate this fact.

References

1. Volm M, Mattern J. Resistance mechanisms and their regulation in lung cancer. Crit Rev Oncog 1996;7:227–44.
2. Gottesman MM, Fojo T, Bates SE. Multidrug resistance in cancer: role of ATP-dependent transporters. Nat Rev Cancer 2002;2:48–58.
3. Wishart GC, Bissett D, Paul J, et al. Quinidine as a resistance modulator of epirubicin in advanced breast cancer: mature results of a placebo-controlled randomized trial. J Clin Oncol 1994;12:1771–7.
4. Rahman A, Husain SR, Siddiqui J, et al. Liposome-mediated modulation of multidrug resistance in human HL-60 leukemia cells. J Natl Cancer Inst 1992;84:1909–15.

Published OnlineFirst April 21, 2009; DOI: 10.1158/0008-5472.CAN-08-2747

5. Booser DJ, Esteva FJ, Rivera E, et al. Phase II study of liposomal annamycin in the treatment of doxorubicin-resistant breast cancer. Cancer Chemother Pharmacol 2002;50:6–8.

6. Soma CE, Dubernet C, Barratt G, et al. Ability of doxorubicin-loaded nanoparticles to overcome multidrug resistance of tumor cells after their capture by macrophages. Pharm Res 1999;16:1710–6.

7. Wong HL, Rauth AM, Bendayan R, et al. A new polymer-lipid hybrid nanoparticle system increases cytotoxicity of doxorubicin against multidrug-resistant human breast cancer cells. Pharm Res 2006;23:1574–85.

8. Wong HL, Bendayan R, Rauth AM, Xue HY, Babakhanian K, Wu XY. A mechanistic study of enhanced doxorubicin uptake and retention in multidrug resistant breast cancer cells using a polymer-lipid hybrid nanoparticle system. J Pharmacol Exp Ther 2006;317:1372–81.

9. Chavanpatil MD, Patil Y, Panyam J. Susceptibility of nanoparticle-encapsulated paclitaxel to P-glycoprotein-mediated drug efflux. Int J Pharm 2006;320:150–6.

10. Minko T, Kopeckova P, Pozharov V, Kopecek J. HPMA copolymer bound adriamycin overcomes MDR1 gene encoded resistance in a human ovarian carcinoma cell line. J Control Release 1998;54:223–33.

11. Minko T, Kopeckova P, Kopecek J. Preliminary evaluation of caspases-dependent apoptosis signaling pathways of free and HPMA copolymer-bound doxorubicin in human ovarian carcinoma cells. J Control Release 2001;71:227–37.

12. Kabanov AV, Batrakova EV, Alakhov VY. Pluronic block copolymers for overcoming drug resistance in cancer. Adv Drug Deliv Rev 2002;54:759–79.

13. Minko T, Batrakova EV, Li S, et al. Pluronic block copolymers alter apoptotic signal transduction of doxorubicin in drug-resistant cancer cells. J Control Release 2005;105:269–78.

14. Koziara JM, Lockman PR, Allen DD, Mumper RJ. Paclitaxel nanoparticles for the potential treatment of brain tumors. J Control Release 2004;99:259–69.

15. Koziara JM, Whisman TR, Tseng MT, Mumper RJ. *In-vivo* efficacy of novel paclitaxel nanoparticles in paclitaxel-resistant human colorectal tumors. J Control Release 2006;112:312–9.

16. Ma P, Dong X, Swadley CS, Gupte A, Leggas M, Ledebur HC, et al. Development of idarubicin and doxorubicin solid lipid nanoparticles to overcome Pgp-mediated multiple drug resistance in leukemia. J Biomed Nanotechnol. In press 2009.

17. Dong X, Mattingly CA, Tseng, MT, Cho M, Adams VR, Mumper RJ. Development of new lipid-based paclitaxel nanoparticles using sequential simplex optimization. Eur J Pharm Biopharm. In press 2009.

18. Papazisis KT, Geromichalos GD, Dimitriadis KA, Kortsaris AH. Optimization of the sulforhodamine B colorimetric assay. J Immunol Methods 1997;208:151–8.

19. Smith PK, Krohn RI, Hermanson GT, et al. Measurement of protein using bicinchoninic acid. Anal Biochem 1985;150:76–85.

20. Polli JW, Wring SA, Humphreys JE, et al. Rational use of *in vitro* P-glycoprotein assays in drug discovery. J Pharmacol Exp Ther 2001;299:620–8.

21. Batrakova EV, Li S, Elmquist WF, Miller DW, Alakhov VY, Kabanov AV. Mechanism of sensitization of MDR cancer cells by Pluronic block copolymers: Selective energy depletion. Br J Cancer 2001;85:1987–97.

22. Némati F, Dubernet C, de Verdière AC, et al. Some parameters influencing cytotoxicity of free doxorubicin and doxorubiicn-loaded nanoparticles in sensitive and multidrug resistant leucemic murine cells: incubation time, number of nanoparticles per cell. Int J Pharm 1994;102:55–62.

23. Tomlinson E, Malspeis L. Concomitant adsorption and stability of some anthracycline antibiotics. J Pharm Sci 1982;71:1121–5.

24. de Verdière AC, Dubernet C, Némati F, et al. Reversion of multidrug resistance with polyalkylcyanoacrylate nanoparticles: towards a mechanism of action. Br J Cancer 1997;76:198–205.

25. Bogman K, Erne-Brand F, Alsenz J, Drewe J. The role of surfactants in the reversal of active transport mediated by multidrug resistance proteins. J Pharm Sci 2003;92:1250–61.

26. Kabanov AV, Batrakova EV, Alakhov VY. An essential relationship between ATP depletion and chemosensitizing activity of Pluronic block copolymers. J Control Release 2003;91:75–83.

27. Dong X, Mumper RJ. The metabolism of fatty alcohols in lipid nanoparticles by alcohol dehydrogenase. Drug Dev Ind Pharm 2006;32:973–80.

28. Kaasik A, Safiulina D, Zharkovsky A, Veksler V. Regulation of mitochondrial matrix volume. Am J Physiol Cell Physiol 2007;292:C157–63.

29. Halestrap AP. The regulation of the oxidation of fatty acids and other substrates in rat heart mitochondria by changes in matrix volume induced by osmotic strength, valinomycin and Ca2+. Biochem J 1987;244:159–64.

30. Berridge MV, Herst PM, Tan AS. Tetrazolium dyes as tools in cell biology: new insights into their cellular reduction. Biotechnol Annu Rev 2005;11:127–52.

31. Stowe R, Koening DW, Mishra SK, Piersonb DL. Nondestructive and continuous spectrophotometric measurement of cell respiration using a tetrazolium-formazan microemulsion. J Microbiol Methods 1995;22:283–92.

Cancer Research
The Journal of Cancer Research (1916–1930) | The American Journal of Cancer (1931–1940)

AACR American Association for Cancer Research

Doxorubicin and Paclitaxel-Loaded Lipid-Based Nanoparticles Overcome Multidrug Resistance by Inhibiting P-Glycoprotein and Depleting ATP

Xiaowei Dong, Cynthia A. Mattingly, Michael T. Tseng, et al.

Cancer Res 2009;69:3918-3926. Published OnlineFirst April 21, 2009.